

PGE₂ receptor EP₃ inhibits water reabsorption and contributes to polyuria and kidney injury in a streptozotocin-induced mouse model of diabetes

Ramzi Hassouneh¹ · Rania Nasrallah¹ · Joe Zimpelmann² · Alex Gutsol² · David Eckert¹ · Jamie Ghossein¹ · Kevin D. Burns^{1,2} · Richard L. Hébert¹

Received: 12 November 2015 / Accepted: 19 February 2016 / Published online: 19 March 2016
© Springer-Verlag Berlin Heidelberg 2016

Abstract

Aims/hypothesis The first clinical manifestation of diabetes is polyuria. The prostaglandin E₂ (PGE₂) receptor EP₃ antagonises arginine vasopressin (AVP)-mediated water reabsorption and its expression is increased in the diabetic kidney. The purpose of this work was to study the contribution of EP₃ to diabetic polyuria and renal injury.

Methods Male *Ep₃^{-/-}* (also known as *Ptger3^{-/-}*) mice were treated with streptozotocin (STZ) to generate a mouse model of diabetes and renal function was evaluated after 12 weeks. Isolated collecting ducts (CDs) were microperfused to study the contribution of EP₃ to AVP-mediated fluid reabsorption.

Results *Ep₃^{-/-}*-STZ mice exhibited attenuated polyuria and increased urine osmolality compared with wild-type STZ (WT-STZ) mice, suggesting enhanced water reabsorption. Compared with WT-STZ mice, *Ep₃^{-/-}*-STZ mice also had increased protein expression of aquaporin-1, aquaporin-2, and urea transporter A1, and reduced urinary AVP excretion, but increased medullary V₂ receptors. In vitro microperfusion studies indicated that *Ep₃^{-/-}* and WT-STZ CDs responded to

AVP stimulation similarly to those of wild-type mice, with a 60% increase in fluid reabsorption. In WT non-injected and WT-STZ mice, EP₃ activation with sulprostone (PGE₂ analogue) abrogated AVP-mediated water reabsorption; this effect was absent in mice lacking EP₃. A major finding of this work is that *Ep₃^{-/-}*-STZ mice showed blunted renal cyclooxygenase-2 protein expression, reduced renal hypertrophy, reduced hyperfiltration and reduced albuminuria, as well as diminished tubular dilation and nuclear cysts.

Conclusions/interpretation Taken together, the data suggest that EP₃ contributes to diabetic polyuria by inhibiting expression of aquaporins and that it promotes renal injury during diabetes. EP₃ may prove to be a promising target for more selective management of diabetic kidney disease.

Keywords Aquaporins · Arginine vasopressin · Diabetic kidney disease · Isolated perfused cortical collecting duct · PGE₂/EP₃ receptors · Polyuria · Urine concentrating function

Rania Nasrallah and Ramzi Hassouneh contributed equally to this manuscript.

Electronic supplementary material The online version of this article (doi:10.1007/s00125-016-3916-5) contains peer-reviewed but unedited supplementary material, which is available to authorised users.

✉ Richard L. Hébert
rlhebert@uottawa.ca

¹ Department of Cellular and Molecular Medicine, Kidney Research Centre, Faculty of Medicine, University of Ottawa, 451 Smyth Road, Room 2514, Ottawa, ON, Canada K1H 8M5

² Ottawa Hospital Research Institute, University of Ottawa, Ottawa, ON, Canada

Abbreviations

AQP1	Aquaporin-1
AQP2	Aquaporin-2
AVP	Arginine vasopressin
CD	Collecting duct
CCD	Cortical CD
COX-1	Cyclooxygenase-1
COX-2	Cyclooxygenase-2
FITC	Fluorescein isothiocyanate
FN	Fibronectin
GFR	Glomerular filtration rate
IMCD	Inner medullary collecting duct
Jv	Net fluid reabsorption
PAS	Periodic acid–Schiff
PGE ₂	Prostaglandin E ₂

SLP	Sulprostone
STZ	Streptozotocin
UT-A1	Urea transporter α 1
V2R	Arginine vasopressin receptor 2
WT	Wild-type

Introduction

The earliest renal manifestation of poorly controlled diabetes mellitus is increased urine flow rate or polyuria and a diminished ability to concentrate urine. High tubular glucose concentration is a recognised initiating factor and persistent hyperglycaemia may result in a primary defect in the collecting ducts (CDs) rendering them impermeable to water [1, 2]. The exact cause and consequence is unknown. Renal prostaglandin E_2 (PGE_2) and cyclooxygenase-2 (COX-2) are increased in humans with diabetes and in animal models of diabetes [3–8]. Renal PGE_2 promotes water reabsorption via EP_4 receptors and inhibits reabsorption via EP_1 and EP_3 , but its role in urine formation is not fully understood [9–13].

The EP_3 receptor is of notable importance as it is highly expressed in the CDs [14, 15], where water and urea transport are hormonally controlled by the antidiuretic hormone arginine vasopressin (AVP). PGE_2 and the EP_3/EP_1 agonist sulprostone (SLP) decrease cAMP and water permeability in the rabbit cortical CD (CCD) through both pertussis toxin- and staurosporine-sensitive mechanisms. EP_3 also inhibits membrane targeting of CD aquaporin-2 (AQP2) [9, 10]. Furthermore, inner medullary CDs display decreased AVP-stimulated water and urea permeability in response to PGE_2 [11, 16]. These findings suggest that the kidney may buffer AVP-stimulated water and urea reabsorption through EP_3 . Though AVP-mediated water flow via CD AQP2 is well recognised, nothing is known about the role of EP_3 in regulating aquaporin-1 (AQP1). Cortical AQP1 in proximal tubules contributes to the majority of water reabsorption, and medullary AQP1 in the descending loops of Henle reabsorbs a smaller portion of water, a process that is regulated by the medullary interstitial osmolar gradient [17].

Several animal models have been used to study the role of PGE_2/EP_3 in urine formation. $Ep_3^{-/-}$ mice (also known as $Ptger3^{-/-}$ mice) exhibit similar basal urine osmolality to wild-type (WT) mice [18]. However, inhibition of PGE_2 production by indometacin increases urine osmolality in WT but not $Ep_3^{-/-}$ mice, suggesting that EP_3 contributes to urine concentrating function [18]. Furthermore, genetic deletion of the purinergic receptor reduces lithium-induced polyuria, associated with a marked decrease in medullary EP_3 [19]. PGE_2 acting through EP_3 may therefore modulate urine formation, but only in pathophysiological states. As yet, no study has assessed the role of EP_3 in diabetic polyuria. Therefore, we studied the contribution of PGE_2/EP_3 to diabetic polyuria,

AVP-mediated CCD water reabsorption, urine concentrating function and diabetic injury in $Ep_3^{-/-}$ mice, with or without diabetes induced by streptozotocin (STZ).

Methods

Animals All animal procedures were approved by the University of Ottawa Animal Care Service. Mice were housed two per cage, on a 12 h light–dark cycle, with free access to standard chow and water. $Ep_3^{-/-}$ mice (C57BL/6) were donated by R. M. Breyer (Vanderbilt University) [20]. Male WT C57BL/6 mice were obtained from Charles River (Wilmington, NC, USA). Diabetes was induced in 8-week-old male mice with five daily intraperitoneal injections of 50 mg/(kg body weight) STZ (Sigma-Aldrich, St Louis, MO, USA) or sodium citrate vehicle [21]. Four groups of mice were studied: WT, $Ep_3^{-/-}$, WT-STZ, and $Ep_3^{-/-}$ -STZ; $n = 12$ –15 mice per group. Blood glucose was measured at 4 weeks post injection to confirm hyperglycaemia (≥ 15 mmol/l). Blood was collected when mice were killed for determination of various plasma analytes by IDEXX laboratories (Markham, ON, Canada). See ESM Methods for further details.

Metabolic cages and urine analysis At 10 weeks post STZ administration, mice were placed in metabolic cages with free access to water and food. Twenty-four hour urine output and water intake were recorded following 24 h adaptation. Urine osmolality was determined by freezing point depression (Advanced Model 3MO Plus Osmometer; Advanced Instruments, Norwood, MA, USA). Urine biochemistry was performed by IDEXX laboratories. Twenty-four hour urine albumin was quantified by Mouse Albumin ELISA (Bethyl Labs, Montgomery, TX, USA) and AVP excretion rates were measured using Arg⁸-Vasopressin ELISA (Enzo Life Sciences, Farmingdale, NY, USA) and corrected for 24 h urine output.

Estimation of glomerular filtration rate Glomerular filtration rate (GFR) was estimated in conscious mice, before they were killed, by fluorescein isothiocyanate (FITC)-inulin clearance [22]. Briefly, 5% FITC-inulin (Sigma-Aldrich) dissolved in 0.9% saline (154 mmol/l NaCl) was dialysed overnight and filtered. Mice were injected with 3.74 μ l/(g body weight) of FITC-inulin via the tail vein. Blood was collected at 3, 7, 10, 15, 35, 55 and 75 min from the saphenous vein into heparinised capillary tubes and centrifuged. Samples were buffered in HEPES (500 mmol/l, pH 7.4) and fluorescence was measured (excitation 488 nm/emission 538 nm). GFR was calculated using a two-compartment clearance model [22].

Histology and immunofluorescence Mice were injected with vehicle or STZ then euthanised by decapitation 12 weeks later. Trunk blood was collected for determination of plasma osmolality. Glomerular and mesangial areas (20 glomeruli per mouse) were viewed on periodic acid–Schiff (PAS)-stained sections and CD luminal areas (50 CDs per mouse) were quantified in a blinded manner. The number of nuclear cysts in CD epithelium was quantified by visual inspection. Immunofluorescence was performed on paraffin-embedded sections blocked with 10% donkey serum–1% BSA for 1 h. Sections were incubated with mouse AQP1 (ThermoFisher, Ottawa, ON) or rabbit AQP2 antibody (Sigma-Aldrich). See [ESM Methods](#) for further details.

Western immunoblotting Primary antibodies were applied to nitrocellulose membranes overnight, followed by the respective anti-mouse or anti-rabbit secondary antibody (Promega, Madison, WI, USA), applied for 90 min. Visualisation was done on the AlphaImager System (ProteinSimple, San Jose, CA, USA) with SuperSignal West Pico Chemiluminescent reagents (Fisher, Ottawa, ON, Canada). β -Actin was used as a loading control. Densitometric analysis was performed using ImageJ (NIH, Bethesda, MD, USA). See [ESM Methods](#) for further details.

Quantitative PCR RNA was extracted with TRIzol Reagent (Life Technologies, Carlsbad, CA, USA) as per manufacturer's guidelines and treated with DNase I. EP_{1–4} receptors were measured by quantitative PCR with the ABI Prism 7000 system using specific Taqman probes and primers and One-step RT-PCR master mix [8]. A 6-point standard curve was performed for each run using mouse cortex RNA 4.7–100 ng. Expression was normalised to GAPDH (TaqMan Rodent GAPDH; Applied Biosystems, ThermoFisher, Ottawa, ON, Canada). The stability of GAPDH expression in WT-STZ mouse cortex compared with WT mice was verified by normalisation with 18S and β -actin as internal controls.

Table 1 Ep₃^{-/-}-STZ mice exhibit attenuated polyuria and polydipsia and have improved urine concentrating function despite hyperglycaemia and glucosuria

Variable	WT	Ep ₃ ^{-/-}	WT-STZ	Ep ₃ ^{-/-} -STZ
Plasma glucose (mmol/l)	9.0 ± 1.0	7.8 ± 1.0	27.5 ± 4.0*	26.9 ± 4.0 [†]
Urine glucose (mmol/l)	2.7 ± 0.1	2.1 ± 0.2	135.0 ± 0.1*	136.0 ± 0.1 [†]
Urine output (ml/24 h)	0.6 ± 0.1	0.7 ± 0.1	29.6 ± 2.0*	19.8 ± 2.0 ^{†‡}
Water intake (ml/24 h)	4.2 ± 0.4	3.2 ± 0.4	35.9 ± 2.0*	28 ± 3 ^{†‡}
Plasma osmolality (mOsm/kg)	320 ± 5	328 ± 8	402 ± 20*	356 ± 5 [‡]
Urine osmolality (mOsm/kg)	2,350 ± 200	2,340 ± 100	899 ± 10*	1,164 ± 40 ^{†‡}
Urine Na ⁺ (mmol/l)	142 ± 9	143 ± 10	23.0 ± 0.4*	24.0 ± 0.5 [†]
Urine Cl ⁻ (mmol/l)	247 ± 20	244 ± 10	35.6 ± 0.7*	34.8 ± 1.0 [†]
Urine K ⁺ (mmol/l)	242 ± 20	213 ± 6	35.4 ± 2.0*	36.6 ± 3.0 [†]

Data are means ± SEM; n = 5–15 per group

*p < 0.05 vs WT; [†]p < 0.05 vs Ep₃^{-/-}; [‡]p < 0.05 vs WT-STZ

In vitro microperfusion Mice were euthanised at 12 weeks post STZ administration and CCDs were microdissected for in vitro microperfusions and measurement of net fluid reabsorption (Jv). [³H]Inulin (2775 kBq/ml) was used as a volume marker. In control periods, three collections were made for calculation of basal Jv following 30 min equilibration. Tubules with a negative basal Jv were discarded. AVP (10⁻⁸ mmol/l; Sigma-Aldrich) was added to the bath and three 10 min collections were made. SLP (10⁻⁷ mmol/l; Sigma-Aldrich) was then added with five additional 10 min collections. Mean Jv was calculated from the three highest collections. See [ESM Methods](#) for further details.

Statistics Graphpad Prism (San Diego, CA, USA) was used for data analysis. Values are expressed as means ± SEM. Statistical analysis was done using one-way ANOVA followed by Tukey's post hoc test. Significant difference was set at p < 0.05. Two-way ANOVA was also performed and significance was indicated in the results sections. Samples were randomised within groups. No data were excluded or omitted from reporting. All measured parameters were included in the results section.

Results

Polyuria and urine concentrating function in Ep₃^{-/-}-STZ mice At 12 weeks post STZ, blood glucose was elevated three-fold and urine glucose to about 135 mmol/l. Polyuria and polydipsia were observed in both diabetic groups but were attenuated by 20–35% in Ep₃^{-/-}-STZ mice (only the changes in urine glucose and volume were significant by two-way ANOVA) (Table 1). Urine osmolality was reduced by 50% in diabetic mice, compared with non-diabetic mice, but the reduction was attenuated in Ep₃^{-/-}-STZ mice (1,164 ± 40 mOsm/kg) compared with WT-STZ mice (899 ± 10 mOsm/kg). Plasma osmolality was increased in WT-STZ mice (402 ± 20 mOsm/kg) compared with WT (320 ± 5 mOsm/kg), and reduced back to

356±5 mOsm/kg in $Ep_3^{-/-}$ -STZ mice. This effect was significant by two-way ANOVA. Urine concentrations of sodium, potassium and chloride were decreased by 80–90% in WT-STZ and $Ep_3^{-/-}$ -STZ mice. Plasma analytes were unchanged between WT-STZ and $Ep_3^{-/-}$ -STZ mice, including sodium, potassium, glucose, blood urea nitrogen and creatinine (data not shown).

AQP1 and AQP2 in $Ep_3^{-/-}$ -STZ mice The majority of renal water reabsorption occurs through AQP1 in the proximal tubule [17]. Cortical AQP1 analysed by western blot was reduced by 50% in both STZ groups (Fig. 1a) and was localised to the proximal convoluted tubules (Fig. 2a). AQP1 fluorescence intensity was similarly reduced in the cortex of diabetic mice (Fig. 2b). Neither analysis was significant by two-way ANOVA.

The maintenance of an interstitial osmolar gradient partly depends on AQP1 in the medullary thin descending limbs and vasa recta [17]. Western blot analysis of medullary AQP1 showed a 50% reduction in STZ mice that was abrogated in $Ep_3^{-/-}$ -STZ mice (Fig. 1b). Immunofluorescence analysis showed that AQP1 was increased by 25% in the outer medulla (non-significant) in $Ep_3^{-/-}$ -STZ mice compared with WT-STZ mice, expressed in pars recta of proximal tubules as demonstrated by their tall cuboidal epithelium (Fig. 2c, d). Inner medullary AQP1 was increased by 50% in $Ep_3^{-/-}$ -STZ mice

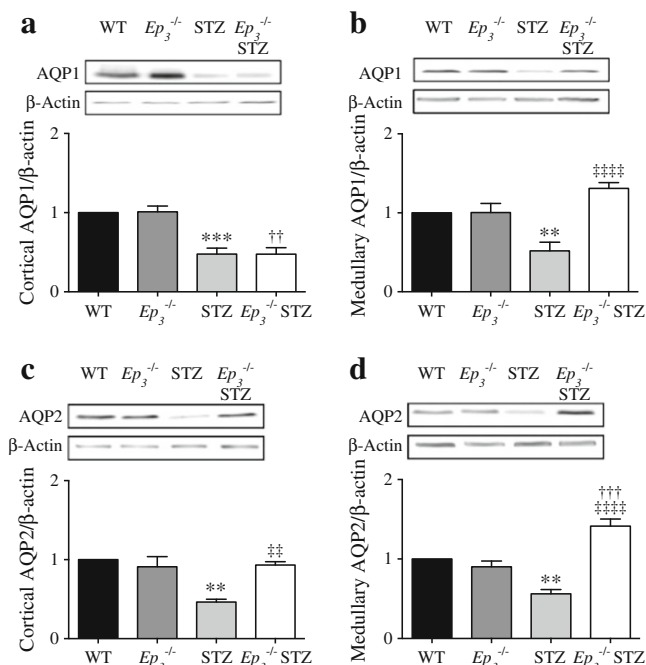


Fig. 1 $Ep_3^{-/-}$ -STZ mice express increased cortical AQP2 and medullary AQP1/AQP2 compared with WT-STZ mice. Representative western blot and densitometric analyses of cortical (a) and medullary AQP1 (b) and cortical (c) and medullary AQP2 (d) in WT, $Ep_3^{-/-}$, WT-STZ (STZ) and $Ep_3^{-/-}$ -STZ mice. Data are presented as fold of WT, means ± SEM, $n=6$. ** $p<0.01$ and *** $p<0.001$ vs WT; †† $p<0.01$ and ††† $p<0.001$ vs $Ep_3^{-/-}$; ††† $p<0.01$ and †††† $p<0.0001$ vs STZ

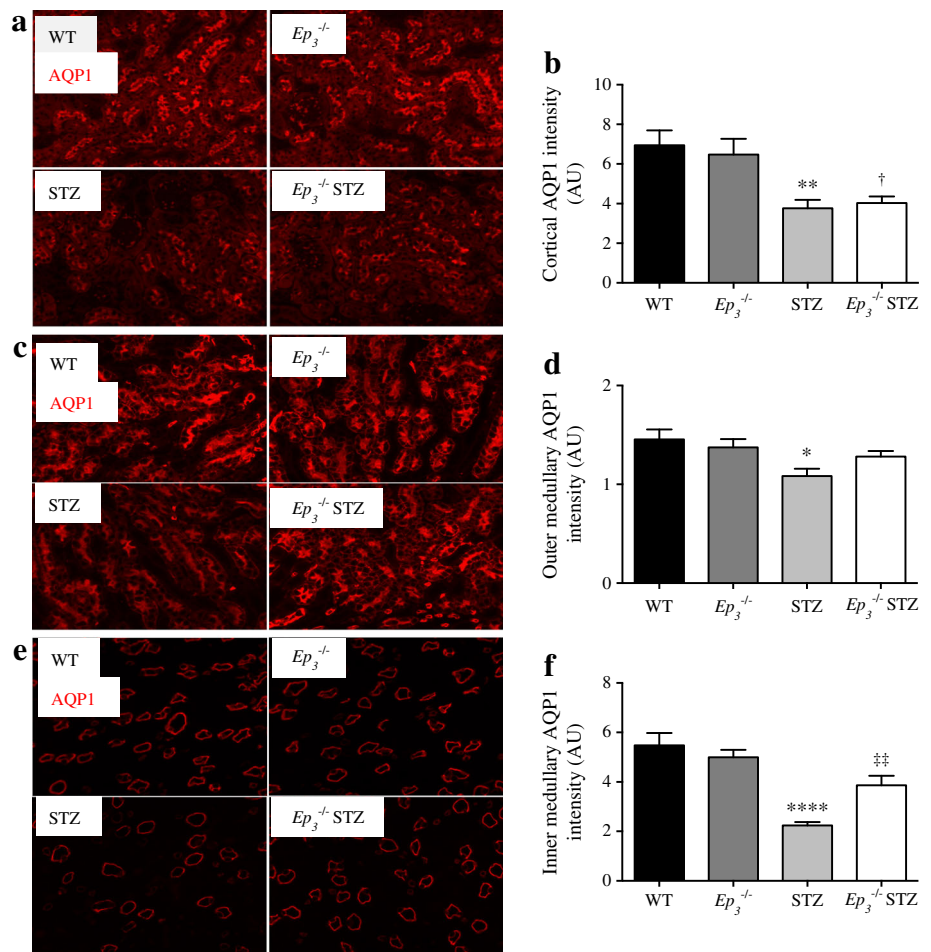
compared with WT-STZ mice, localised to the descending loop of Henle, with squamous epithelium and large lumen (Fig. 2e, f). The medullary changes in AQP1 in both western blot and immunofluorescence analyses were also significant by two-way ANOVA.

AQP2 is hormonally regulated by AVP and mediates CD water reabsorption [17]. Cortical and medullary AQP2, analysed by western blot, decreased by 50% in WT-STZ compared with WT mice (Fig. 1c, d). Cortical AQP2 was increased by 50% (Fig. 1c) and medullary AQP2 was increased threefold in $Ep_3^{-/-}$ -STZ mice compared with WT-STZ (Fig. 1d). We showed the same trends by immunofluorescence, but the magnitude of the increase was greater in the inner medulla (Fig. 3). AQP2 was reduced by 30 and 80% in the cortex and medullary regions of WT-STZ mice compared with WT mice (Fig. 3b, d, f) and was increased by 50% in cortical CDs and threefold in outer medullary CDs of $Ep_3^{-/-}$ -STZ mice compared with WT-STZ mice (Fig. 3a–d). However, AQP2 in inner medullary CDs was elevated fourfold in $Ep_3^{-/-}$ -STZ mice compared with WT-STZ mice (Fig. 3e, f). The changes in AQP2 revealed by western blot and immunofluorescence were all significant by two-way ANOVA.

In vitro microperfusion Since baseline water reabsorption is absent or low in isolated CCDs, AVP was used to stimulate water reabsorption. AVP increased Jv by 70% in both WT and $Ep_3^{-/-}$ mice (Fig. 4a, b). SLP completely reversed the AVP-stimulated Jv in WT mice (Fig. 4a). In $Ep_3^{-/-}$ mice, SLP did not inhibit AVP-stimulated Jv, which remained at 50–70% above baseline (Fig. 4b). In WT-STZ and $Ep_3^{-/-}$ -STZ mice, AVP increased Jv by 70% with respect to baseline (Fig. 4c, d). SLP completely reversed the AVP-stimulated Jv in WT-STZ mice (Fig. 4c) but not $Ep_3^{-/-}$ -STZ mice, where Jv remained elevated at 50–70% above baseline (Fig. 4d). AVP time course experiments were performed on WT CCDs for 80 min following an established baseline for 20 min, and confirmed that the AVP response is maintained at 50–70% above baseline ($p<0.05$; $n=5$) throughout the experimental period

Urinary AVP excretion rate and medullary V2 receptor and urea transporter $\alpha 1$ expression AVP levels are elevated in diabetes despite the presence of polyuria and inability to adequately concentrate urine [1, 23–27]. Since we observed changes in AQP2, which is physiologically regulated by AVP, we measured urinary AVP excretion [17]. WT and $Ep_3^{-/-}$ mice showed a similar urinary AVP excretion rate (207 and 194 pg/24 h, respectively) (Fig. 5a). Both STZ groups exhibited increased AVP excretion rates compared with their vehicle-injected cohorts (2,924 pg/24 h for WT-STZ mice and 1,809, pg/24 h for $Ep_3^{-/-}$ -STZ mice). However, the AVP urinary excretion rate was reduced by 40% in $Ep_3^{-/-}$ -STZ mice

Fig. 2 Inner medullary AQP1 is increased in $Ep_3^{-/-}$ -STZ mice compared with WT-STZ (STZ) mice. Representative image of AQP1 localisation and quantification of AQP1 intensity in cortex (a, b), outer medulla (c, d) and inner medulla (e, f). A minimum of 15 fields of view were assessed per group. Magnification $\times 40$ in (a), $\times 40$ in (c) and $\times 60$ in (e). Data are means \pm SEM, $n=6$. * $p<0.05$, ** $p<0.01$ and **** $p<0.0001$ vs WT; † $p<0.05$ vs $Ep_3^{-/-}$; †† $p<0.01$ vs STZ. AU, arbitrary units



compared with WT-STZ mice (Fig. 5a). This effect was significant by two-way ANOVA.

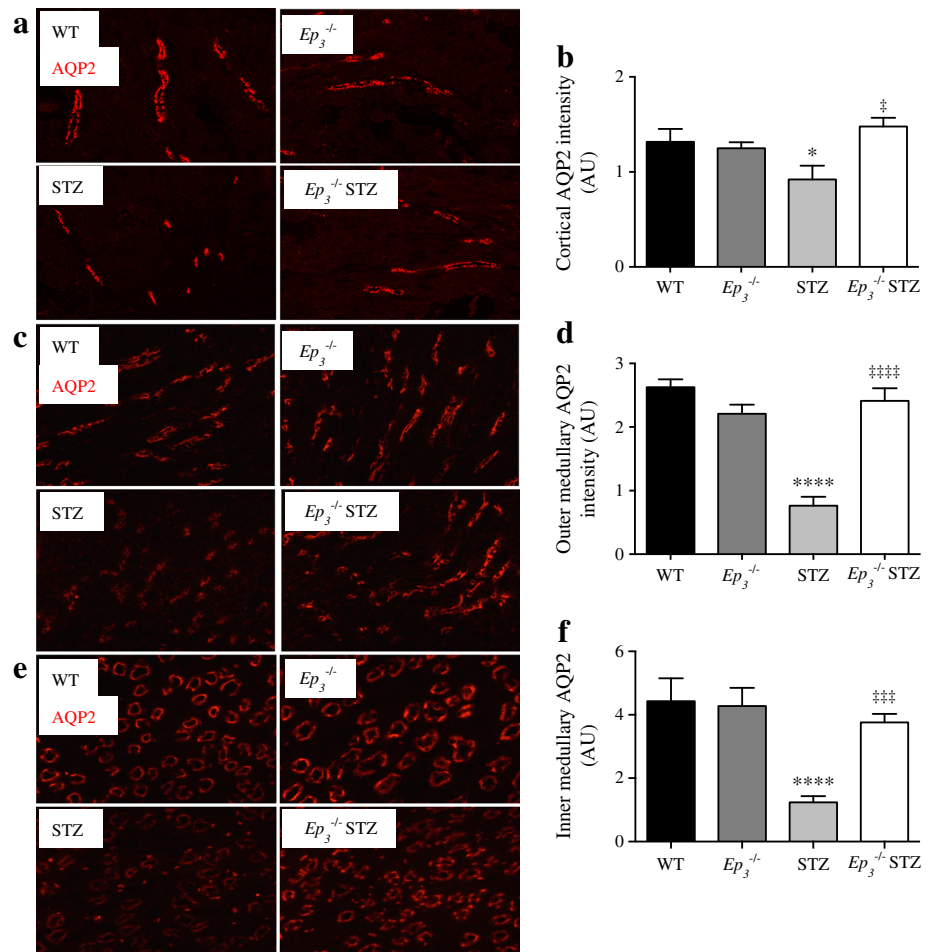
AVP increases water reabsorption and expression of AQP2 by binding to the AVP V2 receptor (V2R) on CD principal cells [17]. Cortical and medullary V2R was increased 50% and 80% in $Ep_3^{-/-}$ -STZ mice, respectively, compared with STZ mice (Fig. 5b, c). AVP can also bind to V2R to increase urea transporter $\alpha 1$ (UT-A1) in the inner medullary collecting duct (IMCD) and consequently increase urea reabsorption, which is necessary to maintain urine concentrating function [28]. Medullary UT-A1 was reduced by 50% in WT-STZ mice compared with WT mice, but was increased threefold in $Ep_3^{-/-}$ -STZ mice compared with WT-STZ mice (Fig. 5d). This effect was significant by two-way ANOVA.

Renal COX-2 and EP receptor expression COX-2 expression is increased in diabetes and contributes to renal functional and structural changes [6–8, 29]. Cortical and medullary cyclooxygenase-1 (COX-1) levels remained unchanged in all groups relative to WT mice (Fig. 6a, b). COX-2 was increased by 50% in the cortex and by 2.5-fold in the medulla of

WT-STZ mice compared with WT mice (Fig. 6c, d). Cortical COX-2 was decreased by 50% and medullary COX-2 by two-fold in $Ep_3^{-/-}$ -STZ mice compared with WT-STZ (Fig. 6d).

Cortical Ep_1 (also known as *Ptger1*) mRNA was expressed at similar levels in all mouse groups but medullary expression was increased twofold in WT-STZ mice compared with WT mice (Fig. 7a). Expression of Ep_1 mRNA was reduced twofold in $Ep_3^{-/-}$ -STZ medulla compared with WT-STZ medulla (Fig. 7a). Cortical and medullary Ep_2 (also known as *Ptger2*) mRNA expression was similar in all groups (Fig. 7b). Cortical Ep_3 mRNA expression was increased by 50%, while medullary Ep_3 mRNA was increased by twofold in WT-STZ mice compared with WT mice (Fig. 7c). Ep_3 mRNA was absent in $Ep_3^{-/-}$ groups. Expression of cortical Ep_4 (also known as *Ptger4*) mRNA was similar in all groups while medullary Ep_4 mRNA expression was increased by 50% in WT-STZ mice (Fig. 7d). As shown in Fig. 7e, we confirmed that GAPDH expression is stable in the cortex of WT-STZ mice compared with WT mice, justifying the use of GAPDH as an internal control in our diabetic studies. As shown, GAPDH expression normalised to 18S or β -actin was similar in WT and WT-STZ mouse cortex.

Fig. 3 Cortical and medullary AQP2 is increased in $Ep_3^{-/-}$ -STZ mice compared with WT-STZ (STZ) mice. Representative image of AQP2 localisation and quantification of AQP2 intensity in cortex (a, b), outer medulla (c, d) and inner medulla (e, f). A minimum of 15 fields of view were assessed per group. Magnification $\times 40$ in (a), $\times 40$ in (c) and $\times 60$ in (e). Data are means \pm SEM, $n = 5$. * $p < 0.05$ and **** $p < 0.0001$ vs WT; † $p < 0.05$, ††† $p < 0.001$ and †††† $p < 0.0001$ vs STZ. AU, arbitrary units



CD dilation and cysts Polyuria has been associated with CD injury, inducing dilation and formation of nuclear cysts in

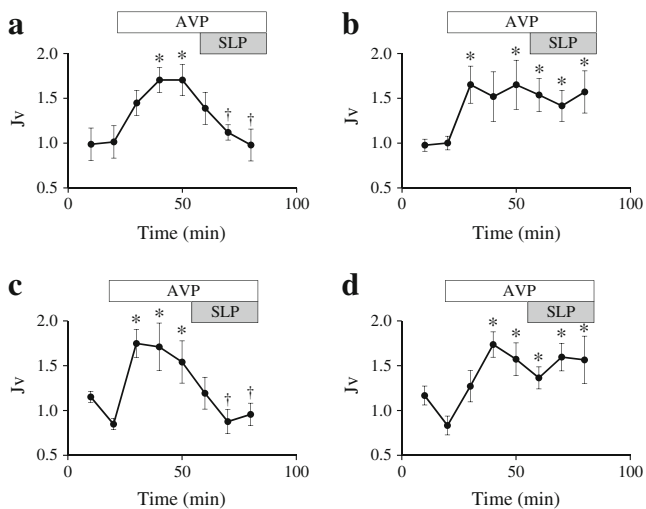


Fig. 4 SLP inhibits AVP-mediated Jv via EP₃. Jv of CCDs isolated from WT (a), $Ep_3^{-/-}$ (b), WT-STZ (c) and $Ep_3^{-/-}$ -STZ mice (d) stimulated with AVP (10⁻⁸ mol/l) and SLP (10⁻⁷ mol/l) presented as fold change of baseline. Data are means \pm SEM, $n = 5$ or 6. * $p < 0.05$ vs baseline at 20 min; † $p < 0.05$ v AVP at 50 min, using an unpaired t test

various models of polyuria [30–32]. As shown in Fig. 8a, CDs were unremarkable with respect to dilation and presence of nuclear cysts in WT and $Ep_3^{-/-}$ mice. Markedly dilated CDs were observed in WT-STZ mice with a twofold increase in luminal area compared with that of the vehicle-injected WT mice (Fig. 8a, b, arrows). CD luminal area remained elevated in $Ep_3^{-/-}$ -STZ mice compared with $Ep_3^{-/-}$ mice; however, the elevation was attenuated by 20% compared with WT-STZ mice (Fig. 8a, b). Nuclear cysts were present in the CD lining in both STZ-injected groups, with the incidence being 30% lower in $Ep_3^{-/-}$ -STZ mice (7.97 \pm 1 cysts per field in WT-STZ mice; 5.26 \pm 1 cysts per field in $Ep_3^{-/-}$ -STZ mice; Fig. 8a, c, asterisk). The effects on CD cysts and dilation were significant by two-way ANOVA.

GFR and renal hypertrophy Increased GFR and urinary albumin excretion are key features of early diabetic kidney disease [33]. As shown in Table 2, WT and $Ep_3^{-/-}$ mice exhibit similar GFRs. GFR was increased by 50% in WT-STZ mice with a twofold increase in urinary albumin excretion. In contrast, GFR was reduced by 20% in $Ep_3^{-/-}$ -STZ mice compared with WT-STZ mice but the reduction in albumin excretion

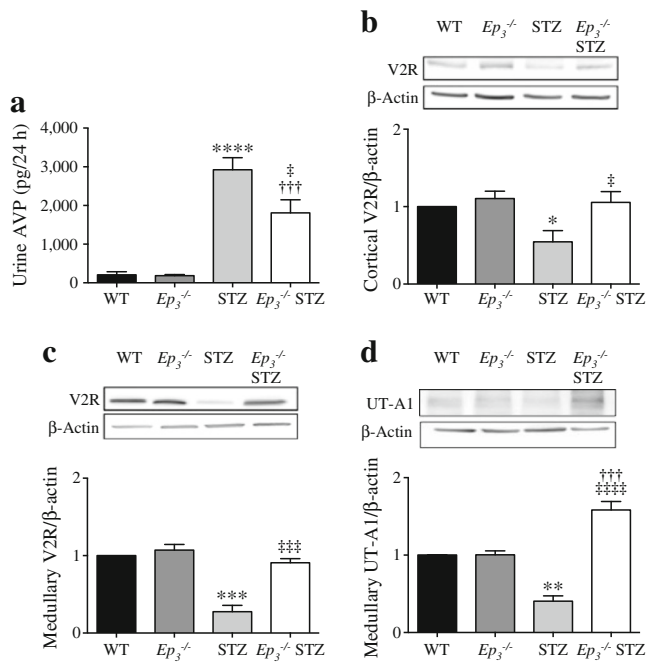


Fig. 5 Urinary AVP excretion rate is decreased while AVP V2R and UT-A1 protein levels are increased in $Ep_3^{-/-}$ -STZ mice compared with WT-STZ (STZ) mice. **(a)** Twenty-four hour urinary AVP excretion. **(b–d)** Representative western blot and densitometric analysis of cortical **(b)** and medullary AVP receptor V2 (V2R) **(c)** and medullary UT-A1 **(d)**. Data are presented as fold WT; means \pm SEM, $n = 6$. * $p < 0.05$, ** $p < 0.01$, *** $p < 0.001$ and **** $p < 0.0001$ vs WT; ††† $p < 0.001$ vs $Ep_3^{-/-}$; † $p < 0.05$, ††† $p < 0.001$ and †††† $p < 0.0001$ vs STZ

rate was non-significant (Table 2). The difference in GFR was significant by two-way ANOVA.

Persistent hyperglycaemia and hyperfiltration can lead to glomerular and tubular hypertrophy and consequently overall kidney growth [33]. As shown in Table 2, body weight was reduced by 20% in WT-STZ mice compared with WT mice, and increased by 10% in $Ep_3^{-/-}$ -STZ mice compared with WT-STZ mice. WT and $Ep_3^{-/-}$ mice exhibited similar kidney weight corrected for tibia length (KW/TL), while WT-STZ mice showed a 30% increase in KW/TL compared with WT mice. $Ep_3^{-/-}$ -STZ mice showed a 10% reduction in KW/TL compared with WT-STZ mice. This effect was significant by two-way ANOVA. Glomerular area was increased by 25% in both STZ-injected groups when compared with WT mice (ESM Fig. 1 a, b) but the change in mesangial area was non-significant (ESM Fig. 1 a, c).

We also analysed markers of cell growth and fibrosis. WT and $Ep_3^{-/-}$ mice expressed similar levels of p21, p27, fibronectin (FN) and TGF- β (Fig. 9a–h). Cortical and medullary p21 and p27 were reduced by twofold (Fig. 9a–d) and FN and TGF- β were reduced by 60% in $Ep_3^{-/-}$ -STZ mice compared with WT-STZ mice (Fig. 9e–h). The effects on cortical and medullary p21 and p27 were significant by two-way ANOVA, whereas only those on cortical TGF- β and FN were significant.

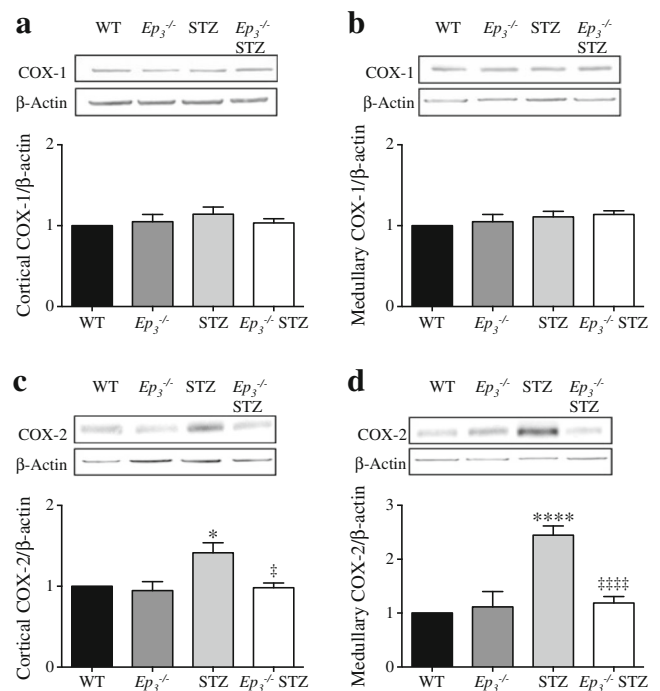


Fig. 6 $Ep_3^{-/-}$ -STZ mice have decreased cortical and medullary COX-2 expression compared with WT-STZ (STZ) mice. Representative western blot and densitometric analyses of cortical **(a)** and medullary **(b)** COX-1 and cortical **(c)** and medullary **(d)** COX-2. Data are presented as fold WT; means \pm SEM, $n = 6$. * $p < 0.05$ and **** $p < 0.0001$ vs WT; † $p < 0.05$ and †††† $p < 0.0001$ vs STZ

Discussion

This study demonstrates the major role of PGE₂ EP₃ receptors in the diabetic kidney and the process of diabetic polyuria. Ep_3 deletion did not affect urine formation in the basal state, but $Ep_3^{-/-}$ -STZ mice display attenuated polydipsia and improved urine and plasma osmolality, suggestive of increased renal water reabsorption. We show that cortical and medullary AQP2 and medullary AQP1 and UT-A1 are reduced in WT-STZ mice and increased in $Ep_3^{-/-}$ -STZ mice, suggesting that the medullary osmolar gradient is maintained. The role of EP₃ in CD fluid reabsorption is confirmed by in vitro tubular perfusion, whereby SLP reverses AVP fluid reabsorption only in $Ep_3^{+/+}$ mice and not in $Ep_3^{-/-}$ mice.

Urinary AVP excretion rate is increased in WT-STZ mice and attenuated in $Ep_3^{-/-}$ -STZ mice, consistent with reports in rodent models of diabetes and in diabetic patients [3–8], presumably to prevent water contraction as a result of persistent polyuria [1, 2]. We propose that PGE₂ acts on EP₃ to buffer AVP. In WT-STZ mice, cortical and medullary COX-2 protein and Ep_3 mRNA are increased, with decreased V2R and reduced CD AQP2. $Ep_3^{-/-}$ -STZ mice have attenuated AVP and COX-2, as well as reduced hyperfiltration and hypertrophy compared with WT-STZ mice, consistent with previous studies of chronic exposure to elevated AVP and COX-2 [3–8]. Our study is the first to show that EP₃ regulates p21 and p27,

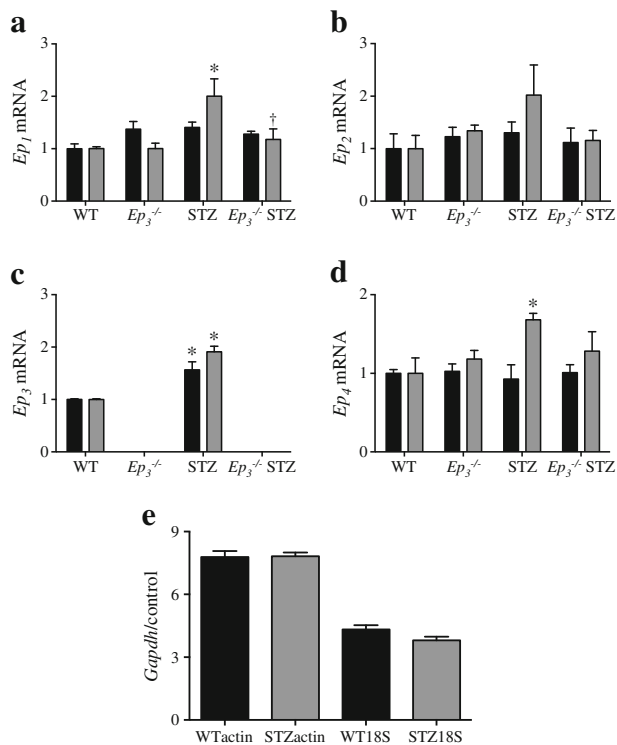


Fig. 7 Medullary EP₁ expression is decreased in *Ep₃^{-/-}*-STZ mice while cortical and medullary EP₃ expression is increased in WT-STZ (STZ) mice. (a–d) Quantitative PCR analysis of cortical (black bars) and medullary (grey bars) EP₁ (a), EP₂ (b), EP₃ (c) and EP₄ mRNA (d) corrected for *Gapdh*. Data are presented as fold vs WT; means ± SEM, n = 6. **p* < 0.05 vs WT and †*p* < 0.05 vs STZ. (e) *Gapdh* in WT and STZ mouse cortex normalised to 18S and β-actin, presented as *Gapdh*/control, means ± SEM, n = 5 for WT and n = 6 for STZ

which are reduced in *Ep₃^{-/-}*-STZ mice compared with WT-STZ mice. TGF-β and FN were reduced in *Ep₃^{-/-}*-STZ mice, suggesting that lower levels of COX-2 and AVP may protect against diabetic injury (growth and fibrosis). EP₂ and EP₄ were reduced in the WT-STZ mouse kidney, consistent with previous findings in STZ mice [8], and are likely not involved in these effects. EP₁ was either unchanged or increased, but in STZ kidneys EP₃ expression was the highest. EP₁ is also likely involved in fibrotic responses, but the overall mechanism may be similar, modulating intracellular calcium directly via EP₁ or indirectly via EP₃, which reduces cAMP leaving calcium unopposed. Future studies will clarify this possibility.

Polyuria, polydipsia and diminished urinary concentrating function are consistently reported in models of diabetes, but studies of renal AQP1 and AQP2 expression are conflicting depending on the species, strain or stage [34–38]. We show that AQP1 and AQP2 are decreased throughout the kidney regions in WT-STZ mice, and this effect is reversed in *Ep₃^{-/-}*-STZ mice. AQP2 effects are greater in the inner medulla, consistent with a predominant presence of principal cells containing AQP2 in the terminal CD. *Ep₃^{-/-}*-STZ mice have a lower urinary AVP concentration than WT-STZ mice, yet enhanced

Table 2 *Ep₃^{-/-}*-STZ mice exhibit attenuated GFR and kidney weight corrected for tibia length

Variable	WT	<i>Ep₃^{-/-}</i>	WT-STZ	<i>Ep₃^{-/-}</i> -STZ
GFR (μl/min)	211 ± 20	240 ± 10	332 ± 10*	269 ± 20†
AER (μg/24 h)	19 ± 3	14.1 ± 4.0	39.3 ± 6.0*	28.2 ± 6.0
KW (mg)	170 ± 7	178 ± 5	211 ± 6*	197 ± 5
KW/TL (mg/m)	9.7 ± 0.3	10.3 ± 0.3	12.4 ± 0.3*	11.1 ± 0.3†
BW (g)	30.7 ± 1.1	34.5 ± 0.9	24.5 ± 0.4*	26.6 ± 0.7†

Data are means ± SEM, n = 5–15 per group

**p* < 0.05 vs WT; †*p* < 0.05 vs *Ep₃^{-/-}*

AER, albumin excretion rate; BW, body weight; KW, kidney weight; TL, tibia length

water reabsorption, suggesting their principal cells are more sensitive to AVP. WT-STZ mice seem to be resistant to AVP, with increased AVP and polyuria compared with *Ep₃^{-/-}*-STZ mice. Renal V2R expression is reduced in WT-STZ mice compared with WT mice, but is increased in *Ep₃^{-/-}*-STZ mice, suggesting the presence of partial nephrogenic diabetes insipidus, characterised by excessive thirst and excretion of

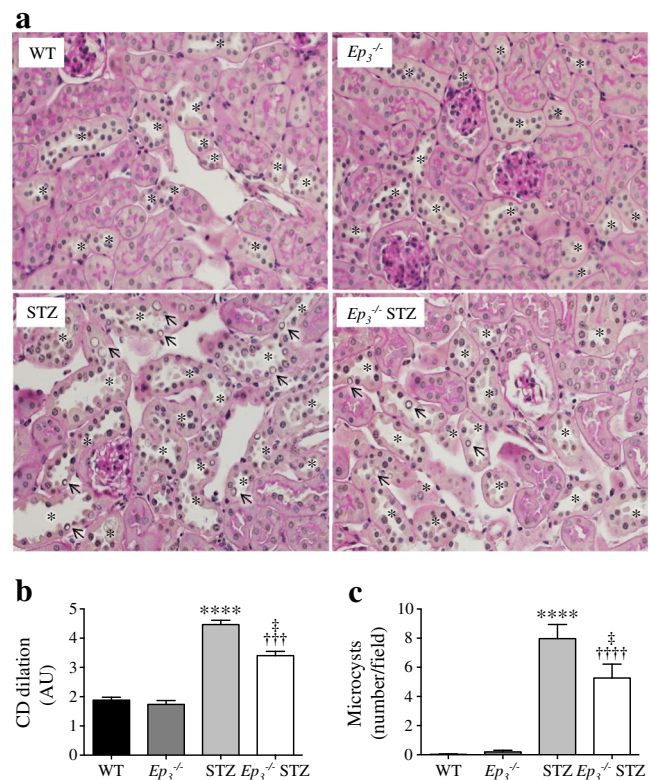


Fig. 8 *Ep₃^{-/-}*-STZ mice have attenuated dilated CDs and epithelial cysts compared with WT-STZ mice. (a) Representative images of CDs obtained from PAS-stained sections. Arrows indicate CD epithelial cysts; asterisks indicate CD dilation. Magnification ×10. (b) Quantification of CD dilation. (c) Quantification of CD epithelial cysts. A minimum of 15 fields of view were assessed per group. Data are means ± SEM, n = 6. *****p* < 0.0001 vs WT; †††*p* < 0.001 and ††††*p* < 0.0001 vs *Ep₃^{-/-}*; ‡*p* < 0.05 vs STZ. AU, arbitrary units

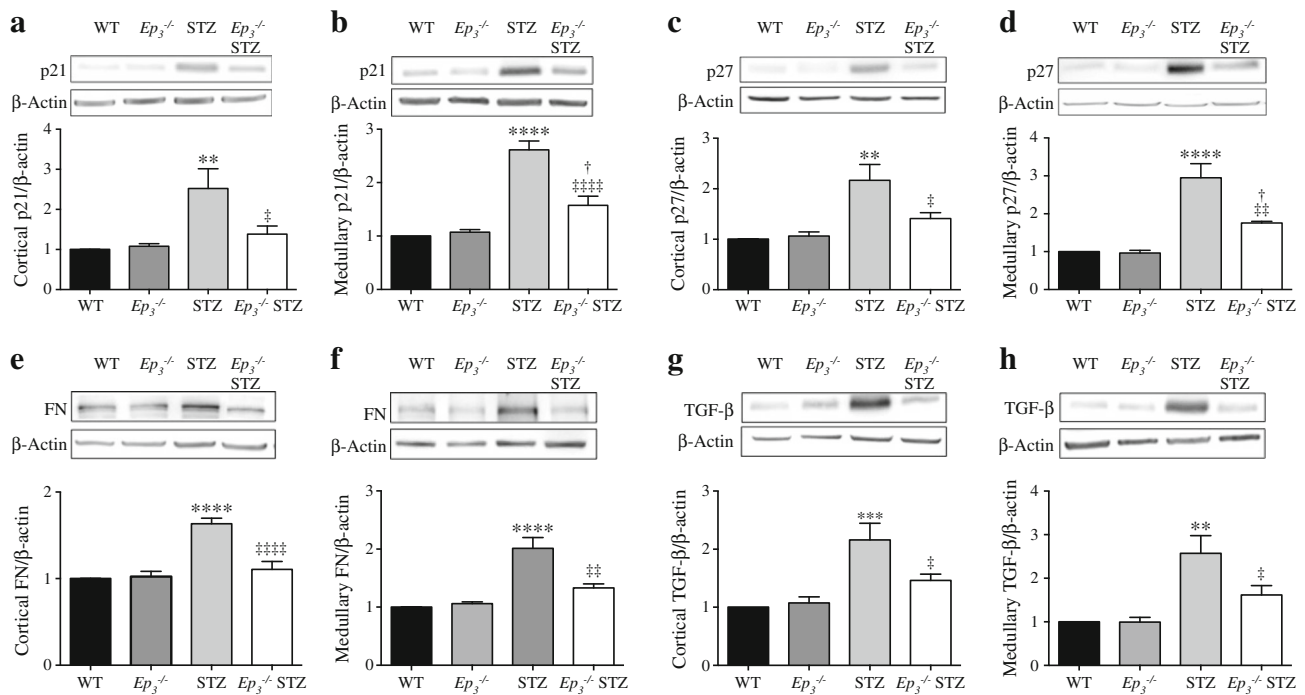


Fig. 9 *Ep3*^{-/-}STZ mice have decreased cortical and medullary p21, p27, TGF-β and FN levels compared with WT-STZ (STZ) mice. Representative western blot and densitometric analyses of cortical and medullary p21 (a, b), p27 (c, d), FN (e, f) and TGF-β (g, h). Data are

presented as fold WT; means ± SEM, $n = 6$. ** $p < 0.01$, *** $p < 0.001$ and **** $p < 0.0001$ vs WT; † $p < 0.05$ vs *Ep3*^{-/-}; ‡ $p < 0.05$, †† $p < 0.01$ and ††† $p < 0.0001$ vs STZ

large amounts of severely dilute urine due to insensitivity of the kidneys to AVP. AVP is secreted in response to osmotic stimuli [1, 2, 39], but when diabetic patients were infused with hypertonic saline, their urine osmolality remained low when compared with non-diabetic individuals despite comparable plasma AVP, suggesting renal resistance to the antidiuretic actions of AVP [1]. Furthermore, when compared with non-diabetic individuals, diabetic patients infused intravenously with AVP had severely reduced urine osmolality and urinary AQP2 [40]. Persistent upregulation of EP₃ reduces V2R and AQP2 in STZ mice, whereas AQP2 is maintained in *Ep3*^{-/-}STZ mice since V2R are restored to WT levels, indicating that EP₃ is responsible for renal resistance to AVP.

EP₃ agonism inhibited CCD AVP-stimulated J_v, as reported in rabbit CCDs [9, 10]. However, greater changes in AQP1, AQP2 and V2R were noted in the medulla than in the cortex. Others have also observed larger AVP-mediated water responses in rat IMCDs compared with rodent CCDs, possibly due to species differences [11, 18, 41]. *Ep3*^{-/-}STZ mice show increased medullary AQP2 compared with WT-STZ and *Ep3*^{-/-} mice, suggesting an enhanced sensitivity to AVP. Immunohistochemistry demonstrates that AQP2 is increased in IMCD. We also show increased medullary AQP1 in *Ep3*^{-/-}STZ mice, whereas cortical AQP1 is reduced equivalently in both diabetic groups. Proximal tubule AQP1 contributes to the majority of water reabsorption in the kidney [17]. Cortical AQP1 is reduced in both STZ-

injected groups concomitant with polyuria, suggesting its role in diabetic polyuria. AQP1 in the descending loop of Henle is responsible for less water reabsorption, and is regulated by the medullary interstitial osmolar gradient [17]. We show enhanced UT-A1 expression in *Ep3*^{-/-}STZ mice, suggesting increased urea recycling from the IMCD into the interstitium. UT-A1 is also regulated by AVP, and its increase is likely due to increased V2R, consistent with a study showing decreased AVP-induced urea permeability in PGE₂-stimulated IMCD [16]. Medullary AQP1 was increased in our study, particularly in the descending loops of Henle of the inner medulla. Therefore, we conclude that *Ep3*^{-/-}STZ mice have improved urine concentrating function due to enhanced urea recycling and increased AQP1 in nephron loops.

Increased COX-2 has been linked to hyperfiltration, hypertrophy and albuminuria in various rodent models of diabetes [3–8] and COX-2 inhibitors prevent these features [3, 5–7]. COX-2 is reduced in *Ep3*^{-/-}STZ mice, with attenuated hyperfiltration and hypertrophy and reduced markers of cell growth (p21 and p27) and fibrosis (TGF-β and FN). Long-term induction of AVP has also been linked to nephropathy [42]. For example AVP-deficient STZ-Battleboro rats were resistant to hyperfiltration, albuminuria and hypertrophy [42]. *Ep3*^{-/-}STZ mice have lower urinary levels of AVP and this may protect against hyperfiltration and renal hypertrophy.

Prolonged polyuria can be damaging to CDs that physiologically do not encounter high flow rates [2]. WT-STZ mice had severely dilated CD lumens; the dilation was reduced in $Ep_3^{-/-}$ -STZ mice correlative to their attenuated polyuria. The WT-STZ mice also exhibited a large number of nuclear cysts in the dilated CDs, with this number being reduced in $Ep_3^{-/-}$ -STZ mice. Similar structural changes have been reported in STZ-diabetic rats and other polyuric diseases including lithium-induced polyuria [30, 43, 44]. This damage may be due to increased flow and expression of paracrine mediators including PGE₂ [44]. AVP inhibits cystogenesis in animal models of polycystic kidney disease by downregulating cAMP, cell proliferation and fluid secretion [45]. Attenuated urinary AVP in $Ep_3^{-/-}$ -STZ mice may account for the reduction in cysts compared with STZ mice.

In summary, PGE₂ and COX-2 regulate urine output in pathological polyuric states. This is the first study demonstrating a role for COX-2/PGE₂/EP₃ in diabetic polyuria. EP₃ is upregulated during diabetes mellitus and thus actively opposes water reabsorption, contributing to polyuria. Although urinary AVP is increased in WT-STZ mice, these mice are polyuric and cannot concentrate their urine. Resistance of WT-STZ mice to renal AVP might be mediated by EP₃ which reduces V2R levels. Since polyuria is an early manifestation of diabetes, it presents a lucrative target to prevent disease progression. EP₃ regulates renal AVP and COX-2, both implicated in early renal injury including enlargement, hyperfiltration and albuminuria. Deletion of EP₃ recapitulates many features of coxib treatment as well as V2R inhibition in early diabetic nephropathy. This highlights the potential benefit of antagonising EP₃ as a more-targeted therapy in diabetes.

Funding This research was supported by the Kidney Foundation of Canada (KFoC No. 550826) and the Canadian Institutes for Health Research (CIHR No. 220694).

Duality of interest The authors declare that there is no duality of interest associated with this manuscript.

Contribution statement All authors contributed to the conception and design of the experiments and performed the experiments, analysed data, prepared figures and drafted manuscript. All authors approved the final version of manuscript. RLH is responsible for the integrity of the work as a whole and is the guarantor of this work

References

- Wang S, Mitu GM, Hirschenberg R (2008) Osmotic polyuria: an overlooked mechanism in diabetic nephropathy. *Nephrol Dial Transplant* 23:2167–2172
- Marsh DJ, Martin CM (1975) Effects of diuretic states on collecting duct fluid flow resistance in the hamster kidney. *Am J Physiol* 229:13–17
- Cherney DZI, Miller J, Scholey JW et al (2008) The effect of cyclooxygenase 2 inhibition on renal hemodynamic function in humans with type 1 diabetes mellitus. *Diabetes* 57:688–695
- Cherney DZ, Reich HN, Jiang S et al (2012) Hyperfiltration and effect of nitric oxide inhibition on renal and endothelial function in humans with uncomplicated type 1 diabetes mellitus. *Am J Physiol Regul Integr Comp Physiol* 303:R710–R718
- Cherney DZI, Scholey JW, Nasrallah R et al (2008) Renal hemodynamic effect of cyclooxygenase 2 inhibition in young men and women with uncomplicated type 1 diabetes mellitus. *Am J Physiol Renal Physiol* 294:F1336–F1341
- Nasrallah R, Robertson SJ, Hébert RL (2009) Chronic COX inhibition reduces diabetes-induced hyperfiltration, proteinuria, and renal pathological markers in 36-wk B6-Ins2 (Akita) mice. *Am J Nephrol* 30:346–353
- Nasrallah R, Robertson SJ, Karsh J, Hébert RL (2013) Celecoxib modifies glomerular basement membrane, mesangial area and podocyte structure in OVE26 mice, but ibuprofen is more detrimental. *Clin Sci* 124:685–694
- Nasrallah R, Xiong H, Hébert RL (2007) Renal prostaglandin E₂ receptor (EP) expression profile is altered in streptozotocin and B6-Ins2Akita type 1 diabetic mice. *Am J Physiol Renal Physiol* 292:F278–F284
- Hébert RL, Jacobson HR, Fredin D, Breyer MD (1993) Evidence that separates PGE₂ receptors modulate water and sodium transport in rabbit cortical collecting duct. *Am J Physiol* 265:F643–F650
- Hébert RL, Jacobson HR, Breyer MD (1990) PGE₂ inhibits AVP-induced water flow in cortical collecting ducts by protein kinase C activation. *Am J Physiol* 259:F318–F325
- Nadler SP, Zimpelmann JA, Hébert RL (1992) PGE₂ inhibits water permeability at a post-cAMP site in rat terminal inner medullary collecting duct. *Am J Physiol* 262:F229–F235
- Li JH, Chou CL, Li B et al (2009) A selective EP₄ PGE₂ receptor agonist alleviates disease in a new model of X-linked nephrogenic diabetes insipidus. *J Clin Invest* 119:3115–3126
- Olesen ET, Rutzler MR, Moeller HB, Praetorius HA, Fenton RA (2011) Vasopressin-independent targeting of aquaporin-2 by selective E-prostanoid receptor agonists alleviates nephrogenic diabetes insipidus. *Proc Natl Acad Sci U S A* 108:12949–12954
- Breyer MD, Jacobson HR, Davis LS, Breyer RM (1993) In situ hybridization and localization of mRNA for the rabbit prostaglandin EP₃ receptor. *Kidney Int* 44:1372–1378
- Breyer MD, Davis L, Jacobson HR, Breyer RM (1996) Differential localization of prostaglandin E receptor subtypes in human kidney. *Am J Physiol* 270:F912–F918
- Rouch AJ, Kudo LH (2000) Role of PGE₂ in alpha2-induced inhibition of AVP- and cAMP-stimulated H₂O, Na⁺, and urea transport in rat IMCD. *Am J Physiol Renal Physiol* 279:F294–F301
- Nielsen S, Frokiaer J, Marples D, Kwon T-H, Agre P, Knepper MA (2002) Aquaporins in the kidney: from molecules to medicine. *Physiol Rev* 82:205–244
- Fleming EF, Athirakul K, Oliverio MI et al (1998) Urinary concentrating function in mice lacking EP₃ receptors for prostaglandin E₂. *Am J Physiol* 275:F955–F961
- Zhang Y, Pop IL, Carlson NG, Kishore BK (2012) Genetic deletion of the P2Y₂ receptor offers significant resistance to development of lithium-induced polyuria accompanied by alterations in PGE₂ signaling. *Am J Physiol Renal Physiol* 302:F70–F77
- Ceddia RP, Lee D, Maulis MF et al (2016) The PGE₂ EP₃ receptor regulates diet-induced adiposity in male mice. *Endocrinology* 157:220–232
- Qi Z, Fujita H, Jin J et al (2005) Characterization of susceptibility of inbred mouse strains to diabetic nephropathy. *Diabetes* 54:2628–2637
- Qi Z, Whitt I, Mehta A et al (2004) Serial determination of glomerular filtration rate in conscious mice using FITC-inulin clearance. *Am J Physiol Renal Physiol* 286:F590–F596

23. Walsh CH, Baylis PH, Malins JM (1979) Plasma arginine-vasopressin in diabetic ketoacidosis. *Diabetologia* 16:93–96
24. Kamoi K, Ishibashi M, Yamaji T (1991) Thirst and plasma levels of vasopressin, angiotensin II and atrial natriuretic peptide in patients with non-insulin-dependent diabetes mellitus. *Diabetes Res Clin Pract* 11:195–202
25. Iwasaki Y, Kondo K, Murase T, Hasegawa H, Oiso Y (1996) Osmoregulation of plasma vasopressin in diabetes mellitus with sustained hyperglycemia. *J Neuroendocrinol* 8:755–760
26. Van Itallie CM, Fernstrom JD (1982) Osmolal effects on vasopressin secretion in the streptozotocin-diabetic rats. *Am J Physiol* 242: E411–E417
27. Brooks DD, Nutting DF, Crofton JT, Share L (1989) Vasopressin in rats with genetic and streptozotocin-induced diabetes. *Diabetes* 38: 54–57
28. Fenton RA (2009) Essential role of vasopressin-regulated urea transport processes in the mammalian kidney. *Pflugers Arch* 458: 169–177
29. Nasrallah R, Landry A, Singh S, Sklepowicz M, Hébert RL (2003) Increased expression of cyclooxygenase-1 and -2 in the diabetic rat renal medulla. *Am J Physiol Renal Physiol* 285:F1068–F1077
30. Kjaersgaard G, Madsen K, Marcussen N, Jensen BL (2014) Lithium induces microcysts and polyuria in adolescent rat kidney independent of cyclooxygenase-2. *Physiol Rep* 2:e00202
31. Kjaersgaard G, Madsen K, Marcussen N, Christensen S, Walter S, Jensen BL (2012) Tissue injury after lithium treatment in human and rat postnatal kidney involves glycogen synthase kinase 3 β -positive epithelium. *Am J Physiol Renal Physiol* 302:F455–F465
32. Yang B, Zhao D, Qian L, Verkman AS (2006) Mouse model of inducible nephrogenic diabetes insipidus produced by floxed aquaporin-2 gene deletion. *Am J Physiol Renal Physiol* 291: F465–F472
33. Dronavalli S, Duka I, Bakris GL (2008) The pathogenesis of diabetic nephropathy. *Nat Clin Pract Endocrinol Metab* 4:444–452
34. Nejsum LN, Kwon TH, Marples D et al (2001) Compensatory increase in AQP2, p-AQP2, and AQP3 expression in rats with diabetes mellitus. *Am J Physiol Renal Physiol* 280:F715–F726
35. Bardoux P, Ahloulay M, Le Maout S, Bankir L, Trinh-Trang-Tan MM (2001) Aquaporin-2 and urea transporter-A1 are up-regulated in rats with type I diabetes mellitus. *Diabetologia* 44:637–645
36. Leung JC, Chan LY, Tsang AQ, Tang SC, Lai KN (2005) Differential expression of aquaporins in the kidneys of streptozotocin-induced diabetic mice. *Nephrology* 10:63–72
37. Ward DT, Yau SK, Mee AP et al (2001) Functional, molecular, and biochemical characterization of streptozotocin-induced diabetes. *J Am Soc Nephrol* 12:779–790
38. Ortiz MC, Albertoni Borghese MF, Balonga SE et al (2014) Renal response to L-arginine in diabetic mice. A possible link between nitric oxide system and aquaporin-2. *PLoS One* 9:e104923
39. Thompson CJ, Davis DN, Baylis PH (1989) Effect of blood glucose concentration on osmoregulation in diabetes mellitus. *Am J Physiol* 256:R597–R604
40. McKenna K, Morris AD, Ryan M et al (2000) Renal resistance to vasopressin in poorly controlled type 1 diabetes mellitus. *Am J Physiol Endocrinol Metab* 279:E155–E160
41. Maeda Y, Terada Y, Nonoguchi H, Knepper MA (1992) Hormone and autacoid regulation of cAMP production in rat IMCD subsegments. *Am J Physiol* 263:F319–F327
42. Bardoux P, Martin H, Ahloulay M et al (1999) Vasopressin contributes to hyperfiltration, albuminuria, and renal hypertrophy in diabetes mellitus: study in vasopressin-deficient Brattleboro rats. *Proc Natl Acad Sci U S A* 96:10397–10402
43. Rasch R (1984) Tubular lesions in streptozotocin-diabetic rats. *Diabetologia* 27:32–37
44. Belibi FA, Reif G, Wallace DP et al (2004) Cyclic AMP promotes growth and secretion in human polycystic kidney epithelial cells. *Kidney Int* 66:964–973
45. Wang X, Wu Y, Ward CJ, Harris PC, Torres VE (2009) Vasopressin directly regulates cyst growth in polycystic kidney disease. *J Am Soc Nephrol* 19:102–108